Measurement of Earth Pressures Near Vertical and Horizontal Boreholes during Packer Tests

Haitao Lan[1], and Ian Moore[2]
[1]*Doctoral student, Department of Civil Engineering and GeoEngineering Centre at Queen's - RMC, Queen's University, Kingston, Ontario, K7L 3N6*
[2]*Professor and Canada Research Chair in Infrastructure Engineering, GeoEngineering Centre at Queen's - RMC, Queen's University, Kingston, Ontario, Canada K7L 3N6.*

ABSTRACT

Packer tests in vertical and horizontal boreholes were conducted in sand placed within a test pit. A packer was inserted after the vertical (or horizontal) boreholes were cut by a Shelby Tube. Packer inflation (and deflation) was used to provide loading (and unloading) sequences to simulate borehole expansion. Null gauges were buried in the sand adjacent to the borehole to measure radial, hoop and axial stresses during packer inflation and deflation. For the vertical borehole tests where sand was in dense state, all sensors were buried at the same depth and it was found that increments of axial stresses increased with increasing increments of radial stresses. Stress measurements made with the null gages indicate that increases in radial pressures applied by the packer lead to decreases in hoop stress corresponding to initially elastic soil response. After the soil experienced shear failure, increases in stress associated with plastic behaviour were observed. When unloading, an elastic change in hoop stresses and radial stresses were observed. For the horizontal borehole configuration, tests were conducted where the sand was tested in loose or dense state, and the sensors were buried a distance three times the borehole radius above the crown. Like the stress behaviour observed in the vertical borehole tests, stress increments changes in the axial, hoop and radial stresses were similar to those seen in the horizontal borehole tests. Geo-PIV was used to calculate soil movements for the horizontal borehole tests, monitoring ground movement during packer inflation, though the magnitude of the ground movements was minimal (less than 1 *mm*). These data provide insights into stress changes during pressuremeter testing, a database for future analytical and numerical developments.

RÉSUMÉ

Des essais de compactages dans des forages verticaux et horizontaux ont été effectués dans du sable placé dans une fosse d'essai. Un instrument a été inséré après que les trous de forage verticaux (ou horizontaux) ont été coupés par un tube Shelby. Le gonflage de l'instrument (et le dégonflage) a été utilisé pour fournir des séquences de chargement (et de déchargement) pour simuler l'expansion du trou de forage. Des jauges nulles ont été enterrées dans le sable pour mesurer les contraintes radiales, circonférentielles et axiales autour des trous de forage pendant le gonflement et le dégonflage du packer. Pour les essais de forages verticaux où le sable était dense, les capteurs ont été enterrés à la même profondeur et on a constaté que les augmentations (diminutions) des contraintes axiales augmentaient (diminuaient) avec les incréments (décroissements) des contraintes radiales. Les mesures de contrainte faites avec les jauges nulles indiquent que les augmentations des pressions radiales exercées par le packer entraînent des diminutions de la contrainte circonférentielle correspondant à la réponse du sol initialement élastique. Après que le sol ait subi une rupture par cisaillement, des augmentations de contrainte associées au comportement plastique ont été observées. Lors du déchargement, une variation élastique des contraintes circonférentielles et des contraintes radiales a été observée. Pour les essais horizontaux de forage, le sable était dans un état lâche ou dense, et les capteurs ont été enterrés à trois fois le rayon du trou de forage sur la couronne. Comme le comportement de contrainte observé dans les essais de forage verticaux, les changements dans les contraintes axiales, circulaires et radiales étaient similaires à ceux observés dans les essais horizontaux de forage. La Géo-PIV a été utilisée pour calculer les mouvements du sol à l'aide de la vélocimétrie par image de particules pour les essais horizontaux de forage, en surveillant le mouvement du sol pendant le gonflement du packer, mais l'amplitude des mouvements du sol était minime (moins de 1 *mm*). Ces données fournissent des informations sur les changements de contraintes lors des essais pressiométriques et sur la réponse des changements de pression de la terre, une base de données pour les futurs développements analytiques et numériques.

1 INTRODUCTION

Pressuremeter tests have been widely used in the field to measure different soil parameters (Palmer, 1972; Hughes, et al., 1977; Houlsby et al., 1992; Clarke, 1995). The interpretation of these parameters is mainly based on cavity expansion models (Vesic, 1972; Carter et al., 1986; Yu and Houlsby, 1991 & 1995). A summary of most cavity expansion models has been provided by Yu (2000).

Like pressuremeter tests applied in the field, a series of medium scale experiments involving packer inflation and deflation have been conducted in GeoEngineering Centre at Queen's University. These experiments were undertaken to investigate stress changes around boreholes and experience was used to study mud loss mechanisms during Horizontal Directional Drilling and using closed form solutions for elastic and plastic response of soil surrounding boreholes in soil (Lan, 2018).

In the experiments, a borehole packer was used to apply incremental radial pressures, but without equipment to measure circumferential strain like a normal pressuremeter inside which there are three strain gauges

attached every 120-degree (i.e. without monitoring cross section changes during the experiments). The packer was inserted not only in vertical boreholes but also in the horizontal direction to simulate borehole expansion. More importantly, earth pressure changes in the radial, hoop and axial directions adjacent to the borehole during inflation and deflation of the packer were measured, behaviour that has rarely been reported in the literature.

These tests report on changes of axial, hoop and radial stresses around the boreholes when the packer was inflated or deflated in sequence. These data produce valuable information analogue to the pressuremeter testing and are a database for future analytical and numerical developments.

2 EXPERIMENTAL SETUP

2.1 Pit

All the experiments were conducted in a pit 2 *m* long, 2 *m* wide and 2 *m* deep (Fig.1). The North, South and East sides of the pit are composed of concrete, while the wall on the West side was a temporary structure constructed from timber. The base of the pit was also made of concrete. All the side boundaries were sufficiently stiff to prevent detectable movements during backfilling and testing.

2.2 Sand

Hydro-Sand was used in all these tests. The sand is uniformly graded with the particle size distribution curve shown in Figure 2. Stiffness and strength of the sand has been qualified using triaxial tests and its parameters are shown in Table 1. More details of the sand can be found in Lan (2018).

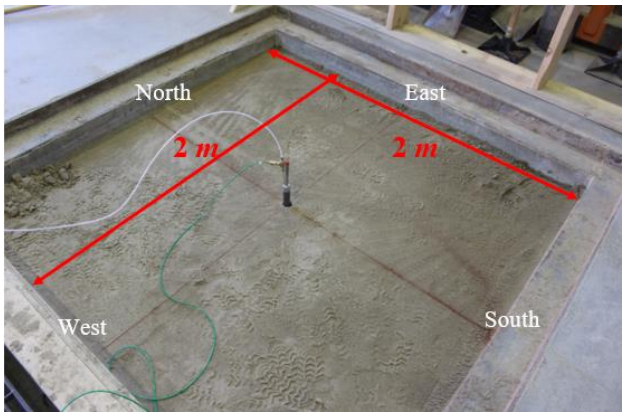

Figure 1. Dimensions of the pit

2.3 Backfilling

During backfilling, Hydro-Sand was placed and compaction of each lift was conducted using two passes of a vibrating plate packer (Wacker WP1550AW with a mass of 88 *kg* and maximum centrifugal force of 15 *kN*). Thickness of each lift was from 200 to 250 *mm*. In each test, earth pressure sensors (null gauges described in the next section) were buried at the same depth during backfilling.

For the vertical borehole experiments, two experiments (Tests VB1 and VB2) are shown here for the sand compacted to a dense state. For the horizontal borehole experiments, two experiments (Tests HB1 and HB2) are also described. The sand was compacted in Test HB1 but not in Test HB2 (though it was still consolidated by body weight during shoveling and leveling in each lift). Information on the test conditions is given in Tables 2 and 3.

Table 1. Parameters of Hydro-Sand

Parameters	Value
Coefficient of Uniformity C_u	3.6
Coefficient of Curvature C_c	1.1
Tangent Elastic Modulus in Loose State (*MPa*)*	$E_i'/p_a = 80.3(\sigma_3'/p_a)^{0.87}$
Tangent Elastic Modulus in Dense State (*MPa*)*	$E_i'/p_a = 405.9(\sigma_3'/p_a)^{0.61}$
Poisson Ratio v	0.3
**Peak Friction Angle ϕ_p'(°)	46
Critical Friction Angle ϕ_c'(°)	35
**Maximum Dilation Angle ψ_{max} (°)	19

* p_a is the atmosphere pressure 101.3 *kPa*; σ_3' is the minimum principal effective stress
**Obtained from Isotropic Consolidated Drained Triaxial Test when $\sigma_3' = 100\ kPa$

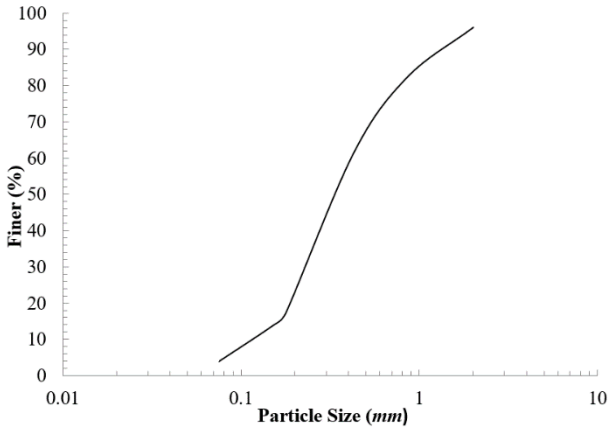

Figure 2. Particle size distribution curve of Hydro-Sand

2.4 Sensors

Null gauges were used to measure axial (vertical stresses adjacent to the vertical boreholes and horizontal stresses for the horizontal boreholes, see Figures 3 and 4), hoop, and radial stresses around the boreholes. The operation of these sensors has been explained by Talesnick (2005). When pressure acts on the sensor, the sensor diaphragm starts to deflect. The deflection is detected by strain gauges attached under the diaphragm and counterbalanced by air pressure added inside the sealed sensor, so the deflection is reduced to a negligible value. LabView (National Instruments) is used to monitor strain and control the air pressure (i.e. to determine the 'nulling pressure'). Because the diaphragm deflection remains negligible, the null gauge

is almost perfectly stiff compared to the surrounding soil, regardless of the soil modulus or loading history, so the calibration remains constant (independent of soil modulus).

Table 2. Parameters in the vertical borehole tests

Test	Average Bulk Density (kg/m^3)	Water Content (%)	Soil Depth (m)	Sensors Depth (m)
VB1 Dense	1842	Not measured*	1.400	0.730
VB2 Dense	1719		1.779	0.500

*Estimated to be 4 to 8%

Table 3. Parameters in the horizontal borehole tests

Test	Average Bulk Density (kg/m^3)	Water content (%)	Sensors Depth (m)	H/D*
HB1 Dense	1710	2.3	0.425	14.2
HB2 Loose	1634	2.6	0.488	15.8

**H* is the distance from ground surface to the springline of the borehole; *D* is the borehole diameter.

For the vertical borehole tests, the centre of each sensor was buried at a distance of three times radius from the centre of the borehole (3*R*), and all were placed at the same burial depth (an example is shown in Figure 3). For the horizontal borehole tests, the sensors were buried above the crown of the boreholes at 3*R* and their locations from Test HB1 are shown in Figure 4.

In addition, during the inflation and deflation steps, nitrogen pressure in the packer was measured by two transducers in two different systems. One was connected to the system used to operate the null gauges and the second was monitored using another data acquisition system. A flowmeter was also connected to the data acquisition system to monitor and record the nitrogen volume and flow rate into the packer during the experiments.

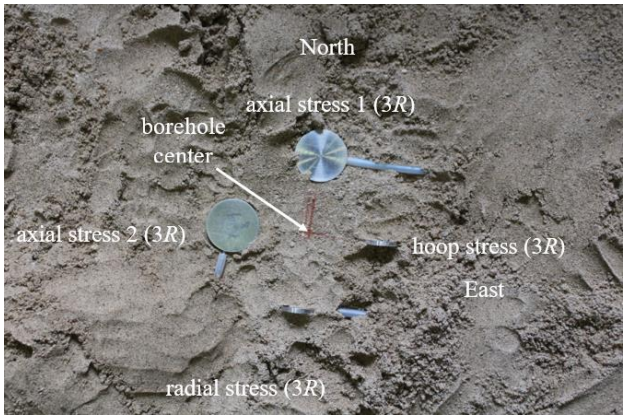

Figure 3. Null gauge locations in Test VB1 during backfilling

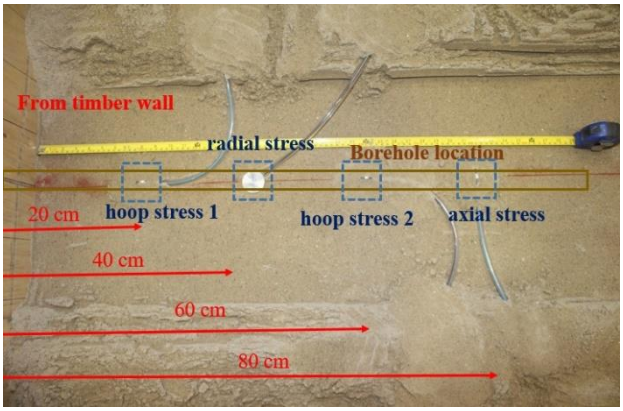

Figure 4. Null gauge locations in Test HB1 during backfilling

2.5 Boreholes and Packer

For the vertical borehole experiments, the borehole was excavated in two ways. Test VB1 used a Shelby tube 1.1 *m* long and with 38 *mm* diameter. In Test VB2, the borehole was drilled using an auger 1.1 *m* long and with 42 *mm* diameter. The centre of the borehole was located in the centre of the pit (Fig.1). For the horizontal borehole experiments, Tests HB1 and HB2, boreholes were cut using the Shelby tube mentioned above. Borehole axis were located 0.4 *m* above the concrete base of the pit. The effective length (*L*) of the borehole was 1 *m* (*L*/*D*≈26).

The packer, manufactured by RST Instruments LTD, featured deflated diameter of 32 *mm* and maximum inflated diameter under unconfined conditions of 71 *mm* under maximum unconfined working pressure of 2.9 *MPa*. It was found that additional friction was introduced during inflation of Test HB1 due to shortening of the packer length. Friction treatment (two polyethylene sheets with silicon grease inside following Tognon et al. (1999)) was then employed around the surface of the packer for the other 3 tests.

During the experiments, the rubber surface of the packer started to fully contact the sand at around 500 *kPa* for borehole diameter of 38 *mm* (diameter of the Shelby tube and borehole), and between 500 and 550 *kPa* when borehole diameter was 42 *mm* (Test VB2, diameter of the auger and borehole).

2.6 Inflation and Deflation

The packer inflation (loading) and deflation (unloading) sequences for Tests VB1 and VB2 are shown in Figure 5. During the loading (and unloading), each load step was held for a few minutes. In Test VB1, the maximum loading pressure actually reached 900 *kPa* but the maximum pressure could not be shown correctly using the transducer connected to the null gauge system. Therefore, in Test VB2, the maximum pressure was reduced to 800 *kPa*.

Like the loading and unloading sequences in the vertical borehole experiments, each loading and unloading step was held for a few minutes in the horizontal borehole experiments. The loading and unloading steps are shown in Figure 6.

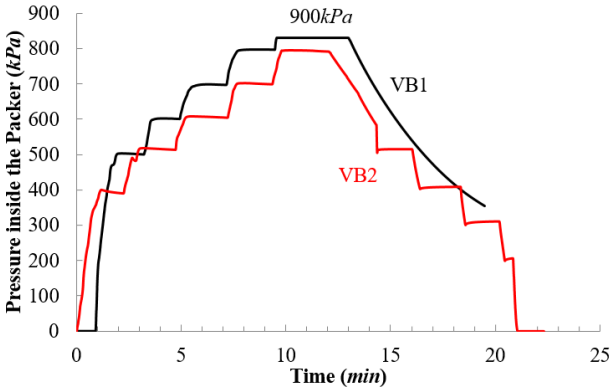

Figure 5. Loading and unloading sequences in the vertical borehole tests

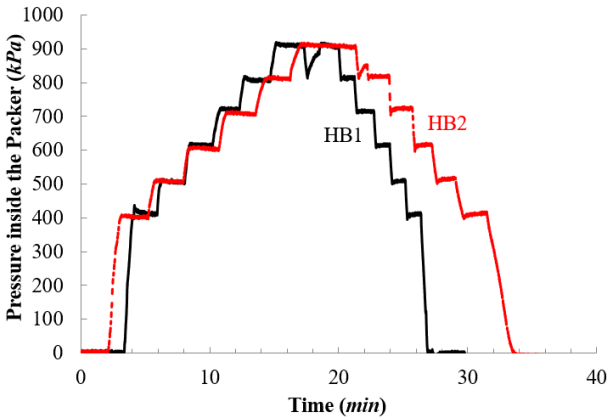

Figure 6. Loading and unloading sequences in the horizontal borehole tests

2.7 Surface Configuration in the Horizontal Borehole Experiments

In Tests HB1 and HB2, the surface of the last lift was carefully leveled. To capture ground movements during packer inflation for the horizontal borehole experiments, numbers of wooden blocks were placed on the surface of the last lift and images were taken by cameras mounted on the South and East walls (Fig.7). A similar setup has been employed in pipe bursting tests in the laboratory (Cholewa et al., 2009) and the field (Brachman et al., 2010).

Square grids (with 100 *mm* by 100 *mm* spacings) were drawn on the ground surface using red chalk lines covering an area 800 *mm* wide and 1100 *mm* long. The *x* axis was designated as the North-South direction while the y axis was the East-West direction. The z axis represents vertical displacement (uplift is considered positive). The digital images were input into the Geo-PIV of White et al. (2003) to calculate the soil movements during testing.

In the tests, the ground movement was minimal (less than 1 *mm*) even when the maximum packer inflation pressure was reached. Therefore, 'pseudo displacements' due to three-dimensional effect were not considered in the calculation process (see Lan, 2018, for more details).

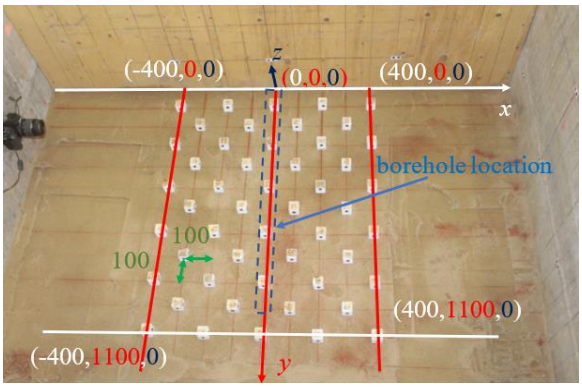

Figure 7. Surface configuration in the horizontal borehole experiments (unit: *mm*)

3 RESULTS AND DISCUSSION

3.1 Vertical Borehole Experiments

The relationships between increments and decrements of hoop stresses and radial stresses in the vertical borehole experiments are shown in Figures 8 and 9. The relationship between increments and decrements of vertical (i.e. axial) and radial stresses in the vertical borehole experiments are shown in Figures 10 and 11.

In Test VB1, when the packer was inflated at 400 kPa (all packer pressures given here are those operating under the rubber, which is not the same as the radial pressure the packer applied to the inside the borehole). The change in earth pressures was minimal because the packer was not yet in full contact with the soil around the borehole. When the pressure reached 500 *kPa*, the hoop stresses began to decrease. Hoop stresses decreased with increasing packer pressure until the packer pressure reached around 700 *kPa*. The trend between the hoop and radial stresses fits expectations for soil responding elastically. As the pressure increased further from 700 to 900 *kPa*, the hoop stresses started to increase, because the soil had begun to experience shear failure, with the stress path following the plastic expansion line (the elastic response line and plastic expansion line are explained in detail by Lan and Moore, 2017).

When the packer began to deflate, hoop stresses initially increased and appeared to track parallel to the elastic response line (over a very small range), then decreased, following the plastic contraction line.

The response of the axial and radial stresses was very different to those for hoop stress. Axial stress path appeared to remain in the elastic range throughout (the loading and unloading lines look very similar). The response measured by the sensor 2 (axial stress 2 shown in Figure 3) in Test VB1 seemed to follow a plastic response line when the pressure passed 800 *kPa*; this is different from the response of the sensor 1 (axial stress 1 shown in Figure 3) (Fig.10). This might be due to different distances between the borehole centre and sensor's location. This distance might a little shorter for the sensor 2 (axis of the borehole could not be perfect at the cross-point show in Figure 3).

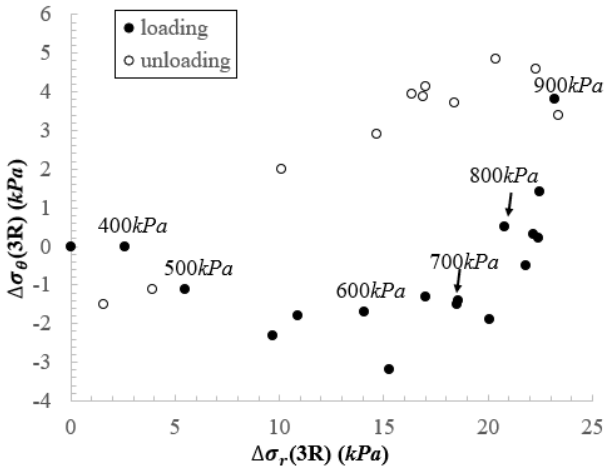

Figure 8. Relationship between increments of hoop ($\Delta\sigma_\theta$) and radial stresses ($\Delta\sigma_r$) in Test VB1

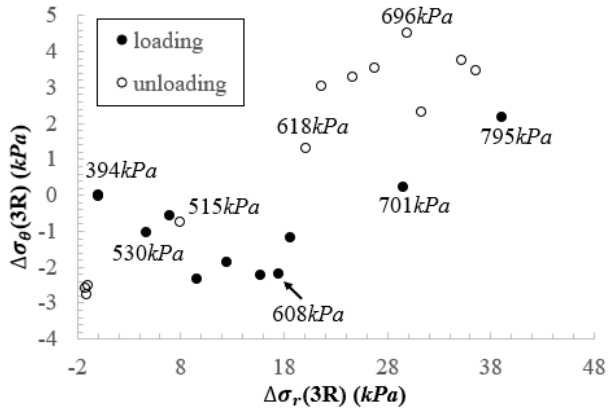

Figure 9. Relationship between increments of hoop ($\Delta\sigma_\theta$) and radial stresses ($\Delta\sigma_r$) in Test VB2

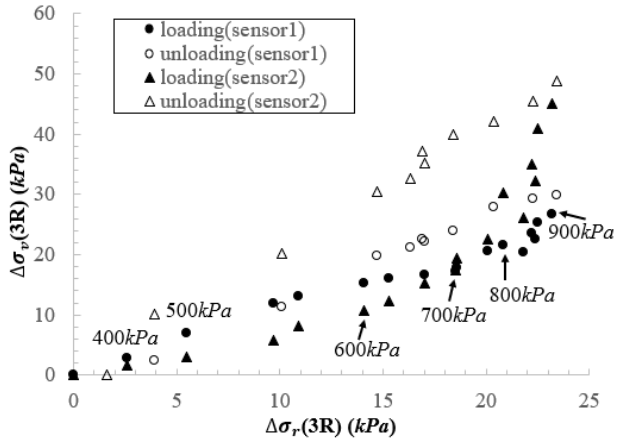

Figure 10. Relationship between increments of axial ($\Delta\sigma_a$ or $\Delta\sigma_v$) and radial stresses ($\Delta\sigma_r$) in Test VB1

Similar behaviour for the hoop and axial stresses and radial stresses can be seen in Test VB2 (Figs.9 and 11).

3.2 Horizontal Borehole Experiments

In the horizontal borehole experiments, many of the features of the relationships between hoop or axial stresses and the radial stresses were similar to those observed for the vertical boreholes.

The main differences are:

- The ranges over which responses were elastic were much smaller when packer inflation commenced (also when packer deflation commenced), see Figures 12 and 13. This is probably related to the smaller confining stresses existing at the sensor locations in the horizontal borehole experiments (the sensor depth was 0.425 m in Test HB1 in contrast to 0.730 m in Test VB1);
- The increments in hoop and axial stresses in Test HB1 (dense state) are larger than those for Test HB2 (loose state), see Figures 12 to 15.

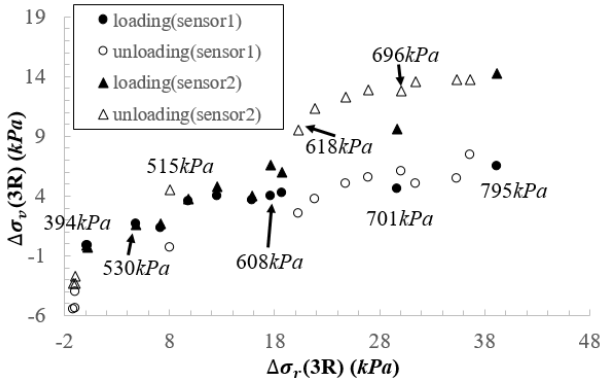

Figure 11. Relationship between increments of axial ($\Delta\sigma_a$ or $\Delta\sigma_v$) and radial stresses ($\Delta\sigma_r$) in Test VB2

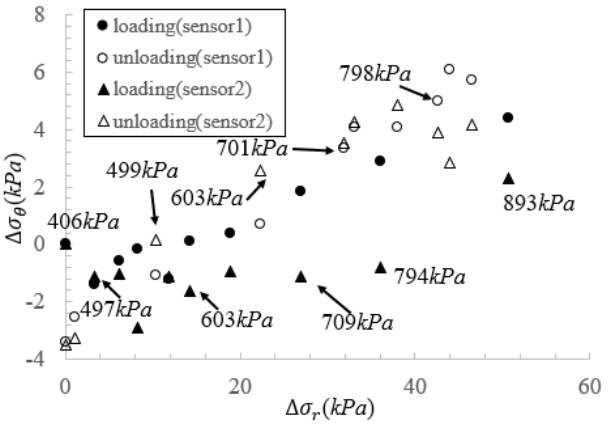

Figure 12. Relationship between increments of hoop ($\Delta\sigma_\theta$) and radial stresses ($\Delta\sigma_r$) in Test HB1

The maximum vertical ground movements are shown in Figures 16 and 17 when the packer pressure reached about 900 *kPa* in Tests HB1 and HB2. The maximum ground movements are seen in the middle of the pit over the packer location, and uplift gradually decreased towards the boundaries of the pit. Though the magnitude was minimal (less than 1 *mm*), differences can still be seen for Tests HB1 and HB2 (i.e. close to 1 *mm* in Test HB1 versus

0.15 *mm* in Test HB2) because in a loose state, the sand is much more compressible than when it is dense.

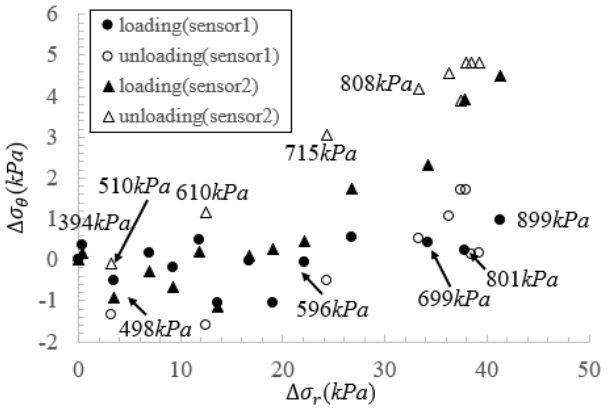

Figure 13. Relationship between increments of hoop ($\Delta\sigma_\theta$) and radial stresses ($\Delta\sigma_r$) in Test HB2

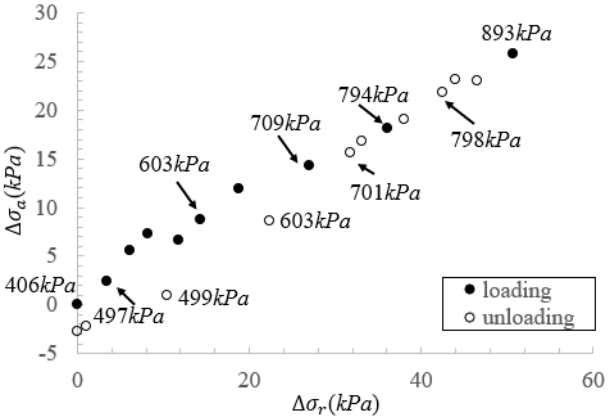

Figure 14. Relationship between increments of axial ($\Delta\sigma_a$) and radial stresses ($\Delta\sigma_r$) in Test HB1

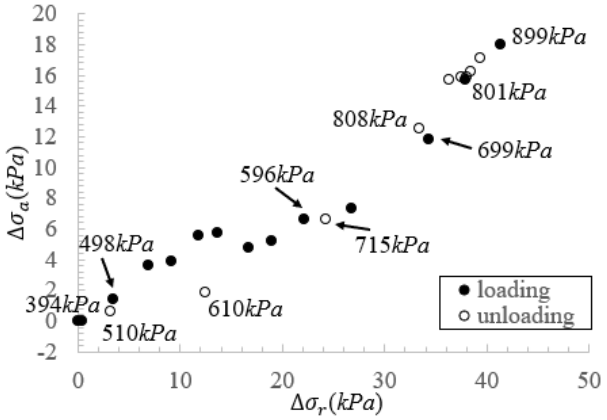

Figure 15. Relationship between increments of axial ($\Delta\sigma_a$) and radial stresses ($\Delta\sigma_r$) in Test HB2

4 CONCLUSIONS

Four packer inflation and deflation experiments were conducted in a pit. Four null gauges were buried in the soil to measure radial, axial and hoop stresses during the loading and unloading process. The purpose of these tests was to investigate whether earth pressures adjacent to boreholes follow stress paths defined by closed form solutions associated with elastic response at intermediate pressures, plastic expansion at high radial pressures, and plastic contraction at low radial pressures (stress paths used in the development of design solutions for mud pressure effects during horizontal directional drilling).

The main findings of the study are:

- The relationship between the increments of hoop stresses and radial stresses fits the expectation, following an initial decrease in hoop stresses as radial stresses increase (i.e. the elastic response line). When the pressure inside the packer continued to increase, shear failure commenced in the soil and the subsequent stress responses followed a plastic expansion line, i.e. the hoop stresses increased as radial stresses increased;
- During unloading, the hoop stresses increased initially, exhibiting an elastic response with gradient similar to the elastic response at the beginning of the inflation process, but that elastic behaviour was restricted to a smaller stress range. When pressure continued to decrease, the response appears to follow the plastic contraction line (since gradient was similar to the plastic expansion line);
- The relationship between increments of axial and radial stresses appeared to be consistently elastic, with response during loading and unloading that was almost the same;
- Similar stress paths were observed in the soil adjacent to vertical and horizontal boreholes. However, the elastic response range in the horizontal borehole expansion experiments was much smaller than that seen for the vertical boreholes;
- The vertical ground movements observed over the horizontal boreholes were much greater when the soil was in a dense state than a loose state; however, all the uplift movements were minimal (less than 1 *mm*).

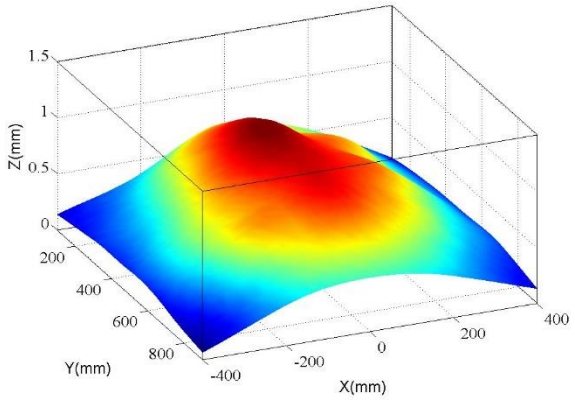

Figure 16. Vertical ground movements in Test HB1

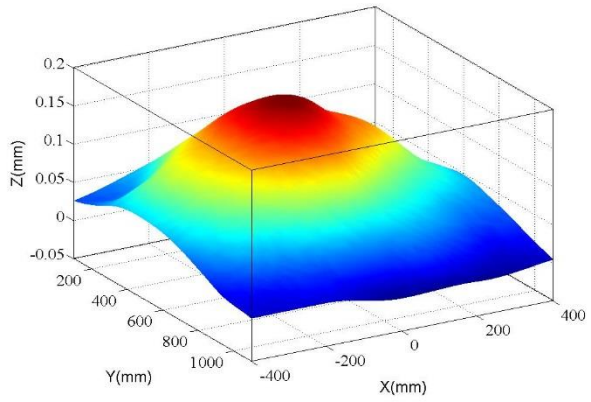

Figure 17. Vertical ground movements in Test HB2

5.REFERENCES

Brachman, R. W. I., McLeod, H. A., Moore, I. D., and Take, W. A. (2010). Three-dimensional ground displacements from static pipe bursting in stiff clay. *Canadian Geotechnical Journal*, 47(4), 439-450.

Cholewa, J. A., Brachman, R. W. I., Moore, I. D., and Take, W. A. (2009). Ground displacements from a pipe-bursting experiment in well-graded sand and gravel. *Journal of Geotechnical and Geoenvironmental Engineering*, 135(11), 1713-1721.

Carter, J. P., Booker, J. Y., and Yeung, S. K. (1986). Cavity expansion in cohesive frictional soils. *Géotechnique*, 36(3), 349-358.

Clarke, B.G. (1995). Pressuremeters in geotechnical design. Blackie Academic & Professional, Glasgow, U.K.

Hughes, J.M.O., Wroth, C.P., and Windle, D. (1977). Pressuremeter Tests in Sands. *Géotechnique*, 27(4), 455-477.

Houlsby, G.T., Carter, J.P. & Yu, H.S. (1992). Report: Studies of the effects of geometry on the results of pressuremeter tests (Report number: OUEL 1928/92). University of Oxford, Oxford, U.K.

Lan, H. (2018). Experimental and numerical investigation of stability of horizontal boreholes during Horizontal Directional Drilling. Ph.D Thesis, Queen's University, Kingston, Ontario, Canada.

Lan, H. & Moore, I.D. (2017). Numerical investigation of the circumferential stresses around boreholes during Horizontal Directional Drilling. *International Journal of Geomechanics*, 17(12), 04017114.

Palmer, A.C. (1972). Undrained plane-strain expansion of a cylindrical cavity in clay: a simple interpretation of the pressuremeter test. *Géotechnique*, 22(3), 451-457.

Talesnick, M. (2005) Measuring soil contact pressure on a solid boundary and quantifying soil arching. *Geotechnical Testing Journal*, 28(2), 171-179.

Tognon, A. R., Rowe, R. K., and Brachman, R. W. (1999). Evaluation of side wall friction for a buried pipe testing facility. *Geotextiles and Geomembranes*, 17(4), 193-212.

Vesic, A.S. (1972). Expansion of cavities in infinite soil mass. *Journal of Soil Mechanics and Foundations Div.*, 98(3), 265-290.

White, D. J., Take, W. A., and Bolton, M. D. (2003). Soil deformation measurement using particle image velocimetry (PIV) and photogrammetry. *Géotechnique*, 53(7), 619-631.

Yu, H. (2000). Cavity expansion methods in geomechanics, Kluwer Academic Publishers, Dordrecht, Netherland.

Yu, H. S., and Houlsby, G. T. (1991). Finite cavity expansion in dilatant soils: loading analysis. *Géotechnique*, 41(2), 173-183.

Yu, H. S., and Houlsby, G. T. (1995). A large strain analytical solution for cavity contraction in dilatant soils. *International Journal for Numerical and Analytical Methods in Geomechanics*, 19(11), 793-811.